Macro- and micro- properties of multi-recycled aggregate concrete

Thomas, C.*[a]; de Brito, J.[b]; Cimentada, A.[a]; Sainz-Aja, J.A.[a]

[1] LADICIM (Laboratory of Materials Science and Engineering), University of Cantabria. E.T.S. de Ingenieros de Caminos, Canales y Puertos, Av./Los Castros 44, 39005 Santander, Spain
[2] CERIS, Instituto Superior Técnico, Universidade de Lisboa, Av. Rovisco Pais, 1049-001 Lisbon, Portugal
* Corresponding author: carlos.thomas@unican.es

Abstract: In a future scenario in which all the concrete is recycled concrete, it will be necessary to recycle the recycled concrete. However, it is known that the recycling of concrete implies a loss of properties. This paper shows an innovative technique, the computerized microtomograph, used to evaluate closed porosity, volume of limestone aggregate fraction and volume of mortar of the multi-recycled aggregate concrete, in order to answer the question: how many times it is possible to recycle concrete? First, the source concrete mix using limestone coarse and fine aggregates was characterized. This mix was crushed to obtain a recycled aggregate that was used to manufacture the 1st generation or current recycled aggregate concrete. After the characterization of this 1st generation concrete, and in the same way, a 2nd and a 3rd generation concrete were obtained and characterized, using recycled aggregates from the 1st and 2nd concrete generations respectively. The evaluation by computerized axial tomography allows to know how the successive recycled affect the properties of the concrete. The results show that it is possible to observe the distribution and quantify the aggregate, cement paste and closed porosity contents of the recycled aggregate concrete showing that 3rd generation recycled concrete shows almost twice as much mortar as 1st generation one and demonstrates that it is only possible to recycle the concrete a finite number of times.

Keywords: Waste; recycled aggregate; recycled aggregate concrete; multiple recycling; adhered mortar; μCT analysis

Acronyms list: computerized microtomograph (μCT); construction and demolition waste (CDW); inter-aggregate propagation mode (InterPM); interfacial transition zone (ITZ); *i*th recycled aggregate concrete (RACi); *i*th recycled aggregate concrete with 25%wt. substitution ratio (RACi-25); limestone fraction of the aggregate (LA); recycled aggregate (RA); recycled aggregate concrete (RAC); saturated surface dry (SSD); scanning electron microscope (SEM); source concrete mix (SC); variable pressure mode (VP); volume of interest (VOI); water/cement (w/c).

1. Introduction

In an historical context, interest on recycled aggregate concrete (RAC) has grown since the 1970s (Buck, 1973; Texas A&M Transportation Institute. PUBL.WKS, 1972). The number of papers has subsequently grown exponentially, as well as their citations, according to the SCOPUS database. The use of recycled aggregate (RA) is thus a topic of high relevance for the scientific community, supported by a growing social need to preserve resources and valorize wastes. In addition, the growing number of researches is a consequence of the large number of issues that have to be resolved before using regularly RAC. The first scientific papers on RAC described methods to incorporate waste in the concrete mix and its feasibility was demonstrated. Between 2000 and 2010, with emphasis on the works of Etxeberria et al., Meyer et al., Xiao et al. and Evangelista et al. (Etxeberria et al., 2007; Evangelista and de Brito, 2007; Meyer, 2009; Xiao et al., 2005), the manufacturing techniques of RA and the compressive strength of RAC began to be described and understood. In the following years (2010-2015), the mechanical and durability performance and the interaction between the

different phases of the composite material are characterized in depth by Silva et al., Kou et al., Kwan et al. and Thomas et al. (Kou and Poon, 2012; Kwan et al., 2012; Silva et al., 2014; Thomas et al., 2013).

There are already structures and precast components that use RAC (Fiol et al., 2018; López Gayarre et al., 2018; Pedro et al., 2017; Thomas et al., 2016) and the use of RA is beginning to be seen as a necessary alternative. In Spain, according to data from ANEFA (ANEFA, 2017), the consumption of aggregates for construction in 2017 (lowest point in the last 10 years) was approximately 2 tonnes per inhabitant, lower than the European yearly average of 5 tonnes per inhabitant. In addition, also in Spain, the generation of construction and demolition waste (CDW) is approximately 1 tonne per inhabitant and year. If one considers that 20% by weight of the 30 million tonnes of CDW, generated in 2017, is structural concrete, the replacement with RA of just 10% by weight of the aggregate used nowadays in construction would be enough to use the 6 million tonnes concrete waste. This suggests a future scenario in which RAC will be used in common practice.

It is for this reason that the CDW of the future will have new and different compositions, i.e. future concrete waste will be formed in part by RAC and consequently the characteristics of the RA will be different. That is why it is necessary to analyze the properties of multi-recycled aggregate and of the concrete containing it. Salesa et al. (Salesa et al., 2017) have analyzed the effect of the multi-recycling of precast elements and showed that the workability and the density decrease with the number of cycles. Therefore, there is a need for quick characterization of the multi-recycled aggregate and concrete.

Chotard et al. (Chotard et al., 2003) showed the importance of the microtomography technology, to analyse cement and concrete composites, demonstrating that hydration starts inside the specimen before spreading all over. Asahina et al. (Asahina et al., 2011) used high-resolution tomography in order to predict the mechanical behaviour of concrete by analyzing the cracking progress. Using microtomography technology, Thomas et al. (Thomas et al., 2018) demonstrated that multi-recycling aggregate increases the volume of adhered mortar and cement paste as the number of cycles goes up. This incorporation of a high volume of adhered mortar in RA causes an increase in water absorption that reduces the effective water/cement (w/c) ratio if it is not compensated by adding extra water. Furthermore, cement paste or adhered mortar are generally less resistant to static (Thomas et al., 2013) and dynamic loading (Oneschkow, 2016; Thomas et al., 2014, 2009) than limestone aggregate. Lanzón et al. (Lanzón et al., 2012) demonstrated that, notwithstanding the limitation of the samples' size used in microtomography, this technic reports coherent results concerning closed porosity. Also, Monteiro et al. (Monteiro et al., 2009) analyzed the durability of concrete exposed to freezing cycles and the alkali–aggregate reaction using microtomography.

However, there is no research is which microtomography is applied in order to analyse multi-recycled aggregate concrete. It is expected that the incorporation of multi-recycled aggregate in concrete implies a reduction of the mechanical properties and it is observed that, from the second cycle, the ratio of coarse limestone fraction in the RA is reduced to 20% by weight (Thomas et al., 2018) so the question is how many times can concrete be recycled?

This paper presents an innovative technique used in the analysis of multi-recycled aggregate concrete. A computerized microtomograph (μCT) was used to evaluate the closed porosity, the volume of the limestone fraction of the aggregate (LA) and the volume of mortar of RAC. To achieve this purpose, a source concrete mix (SC) using limestone coarse and fine aggregates was prepared and characterized with density of 2.51 g/cm^3 and 2.54 g/cm^3 respectively. The SC was crushed to obtain the 1st generation or current recycled aggregate, RA1. After the characterization of this aggregate, a 2nd (RA2) and a 3rd (RA3) generation coarse RA were manufactured and characterized, by crushing concrete made with RA1 and RA2 respectively.

For the characterization of multi-recycled concretes, physical-mechanical characterization tests, tests for the determination of paste/mortar and aggregate volumes by means of tomography, as well as a deep microstrutural study have been carried out. The conducted test responds to the need to confirm that the physical and mechanical properties, such as absorption and compressive strength, of multi-recycled concrete meet the structural requirements. The evaluation by computerized axial tomography allows to know how the successive recycled affect the properties of the concrete. The

97 results show that with this technique it is possible to analyse qualitatively and quantitatively the
98 aggregate, cement paste and closed porosity contents of the recycled aggregate concrete. The same
99 specimen is characterized by other methods and it is also determined how all these parameters are
100 influenced by the number of recycling cycles. A reduction of the size of the coarse LA and an increase
101 of the volume of mortar of the hardened concrete were identified, evaluated and correlated with the
102 number of cycles. The parameter that most influences the properties of multi-recycled concrete is the
103 increase in the volume of mortar adhered to the aggregate with successive recycling. 3rd generation
104 recycled concrete shows almost twice as much mortar as 1st generation one. The impact of this
105 research to the engineering is that it demonstrates that it is only possible to recycle the concrete a
106 finite number of times. From the 3rd generation the produced concrete is basically mortar. However,
107 the number of recycling could increase with equivalent addition of new natural aggregate.

108 **2. Methodology**

109 A total of seven concrete mixes were studied: a SC produced with LA and six RAC using 25%vol.
110 and 100%vol. RA resulting from three different recycling cycles. Crushing SC produced RA1 that was
111 used to make the first recycled aggregate concrete (RAC1). RA2 was obtained by crushing RAC1 and
112 used to make the second recycled aggregate concrete (RAC2). RA3 was obtained by crushing RAC2.
113 The third recycled aggregate concrete (RAC3) was made with RA3. The i^{th} recycled aggregate concrete
114 (RAC*i*) was produced using 100% RA*i*, where *i = 1, 2, 3* depending on the recycling cycle. An
115 incorporation ratio of 25%vol. of coarse RA was used in order to have the results of the most
116 commonly allowed substitution ratio, obtaining RAC*i*-25. The LA and RA*i* were divided in five coarse
117 aggregate fractions (4-5.6 mm, 5.6-8 mm, 8-11.2 mm, 11.2-16 mm and 16-22.4 mm) in order to mix
118 them using the Faury's design method. During the crushing process, the maximum particle size has
119 remained constant and, in a subsequent process, the different fractions have been divided. In each
120 the crushing processes, a reduction on the time and energy invested in the process have been
121 observed. In the crushing process of RAC*i*, the increase of *i* produces more friable particles and the
122 crushing process is accelerated.
123 All the manufactured concretes presented the same grading curve, corresponding to the one
124 proposed by Faury. All the mix proportions were designed with 350 kg/m^3 of Portland cement CEM
125 I 42.5, the same effective w/c ratio (0.55) and slump of 12±1 cm. Table 1 shows the mix proportions
126 used. To offset the fresh concrete workability reduction due to the RA incorporation, the most
127 implemented approach and with the best results in terms of workability is the addition of
128 compensation water (Brito et al., 2019).

129 ***Table 1.*** *Mix proportions (kg/m^3).*

Concrete:	**SC**	**RAC*i***			**RAC*i*-25**		
		***i*=1**	***i*=2**	***i*=3**	***i*=1**	***i*=2**	***i*=3**
Cement:	350	350	350	350	350	350	350
Effective water:	193	193	193	193	193	193	193
Compensation water:	-	10	12	13	40	48	55
Sand (0-2 mm):	732	732	732	732	732	732	732
LA (4-5.6 mm):	97	-	-	-	72	72	72
LA (5.6-8 mm):	107	-	-	-	80	80	80
LA (8-11.2 mm):	116	-	-	-	87	87	87
LA (11.2-16 mm):	327	-	-	-	245	245	245
LA (16-22.4 mm):	327	-	-	-	245	245	245
RA*i* (4-5.6 mm):	-	86	81	79	21	20	72

Concrete:	SC	RAC*i*			RAC*i*-25		
		i=1	*i=2*	*i=3*	*i=1*	*i=2*	*i=3*
RA*i* (5.6-8 mm):	-	95	89	87	24	22	80
RA*i* (8-11.2 mm):	-	103	97	94	25	24	87
RA*i* (11.2-16 mm):	-	293	274	267	73	68	245
RA*i* (16-22.4 mm):	-	292	274	267	73	68	245
Effective w/c:	0.55	0.55	0.55	0.55	0.55	0.55	0.55
Apparent w/c:	0.55	0.67	0.69	0.71	0.58	0.59	0.59

Both the angularity and the water absorption evolve as the number of recycling operations increase. Both of them affect the workability of the mixes. In order to keep the slump or workability, the effective water/cement ratio was adjusted within the range intended. However, the water/cement effective ratio changes were minor but in terms of absolute ratio, the changes were important. The concrete mixes were analyzed using standard 150x300 mm cylindrical specimens cut to obtain subsamples in order to perform the microanalysis.

2.1. Physical and mechanical properties

The specific gravities and closed porosity were analyzed by standard methods (EN-12390-7, 2009) in order to compare the results and validate the μCT technique. For the determination of these parameters, the test dried specimens were subjected to 24 h vacuum, after which water was incorporated (at laboratory temperature) to saturate the accessible porosity, forced by the vacuum. After another 24 h of vacuum saturation process, the vacuum was replaced by atmospheric pressure for another 24 h. Once the test specimens have been saturated, their apparent volume has been evaluated by immersion in water, observing the displaced water volume. The weight of the saturated samples was also registered and then the test specimens were dried inside an oven at 105 ºC to constant weight. The dry weight has been registered. The density and specific gravity have been determined by comparing the dry weight of the sample with the apparent volume and the relative volume, obtained from the apparent volume and the weight of water absorbed. The water absorption coefficient of concrete was obtained by evaluating the open pore volume after saturating it with water using vacuum. The porosity of concrete was obtained as the ratio between volume of accessible porosity and specimen volume. Crushing concrete to powder (with maximum size of 100 μm), the real density was determined using pycnometers. Also, the closed porosity was evaluated as the difference between apparent specific gravity and real density. The difference between bulk specific volume and apparent specific volume provides the open porosity. Also, compressive strength tests (12390-3, 2009; 12390-4, 2001) of each mix at 28 days were performed.

2.2. Computerized microtomography (μCT)

In order to obtain both quantitative and qualitative information on concrete, μCT tests were performed. Valuable information about the volume and distribution of the different material phases of the specimen was thus obtained. The μCT analysis consists of four steps: scanning, reconstruction, qualitative analysis and quantitative analysis. The same analysis configuration was used for all the samples in order to compare the results. During the scanning phase, X-ray images are taken while the sample rotates inside the microtomograph. This scan was made with a Skyscan1172 μCT with an X-ray source of 100 kV of voltage and an amperage of 100 μA. The pixel size was defined as 27 μm. For scanning large samples, their total length is divided in different number of subscans, which will be joined in the reconstruction phase. This consists of the composition of X-ray images to build a 3D digital model of the sample. This composition converts the linear absorption of the materials into a grey scale. In this phase, some corrections such as smoothing, misalignment compensation, ring

artefacts reduction and beam-hardening have been made to improve the analysis. Large sample reconstruction is divided in two different steps: first each of the subscan is reconstructed and, at the end, all the subscans are aligned and combined. In this instance, in order to reduce the reconstruction time, the alignment phase was skipped.

The quantitative analysis provides information about the volume of the different elements inside the sample. In this case, the properties to analyze are the volume of LA, the volume of mortar and the volume of air inside the Volume of Interest (VOI). One of the most interesting quantitative analysis parameters is the volume of coarse RA. To obtain this parameter, the volume of limestone fraction particles with size greater than 4 mm within the different concrete mixes was evaluated. It was thus possible to evaluate how LA turns to sand with the recycling cycles. The volume of air was evaluated by the closed porosity and the size of the pores was also analyzed. The qualitative analysis gives information on the distribution and geometry of the limestone aggregate and the pores.

The concrete samples were cut using a precision cutting saw, from a central area of the standard 150x300 mm cylindrical specimen. The samples obtained for analysis in μCT, are approximately 30x15x15 mm (Fig. 1). For solid samples of concrete, it is advisable not to use samples thicker than 20 mm because of the loss of energy/attenuation of the X-ray, leading to an important loss of resolution.

2.3. Scan electron microscopy

The microscopic examination and analysis of the elemental chemical composition of the samples were carried out using a scanning electron microscope (SEM), Carl Zeiss model EVO MA 15. This equipment uses a lanthanum hexaboride filament as electron source and is provided with secondary and backscattered electron detectors for the generation of images as well as an Oxford Instruments X-ray microanalysis system by energy-dispersive spectrometer (EDS). This SEM can operate in variable pressure mode (VP), with a low vacuum, which enables it to be used for the observation of samples that are non-conducting without the need of metallization. High-vacuum and gold-coated samples were used in order to maximize the resolution of the images (Fig. 1) and VP was used for the analysis of the chemical elemental composition.

The concrete samples were cut using a precision cutting saw, from a central area of each standard cylindrical specimen. The sample obtained for SEM analysis is approximately 40x30x15 mm. The elemental chemical composition of each concrete mix was determined using a sample of approximately 50 g of powder prepared crushing concrete to 100 μm in an agate mortar (Fig. 1).

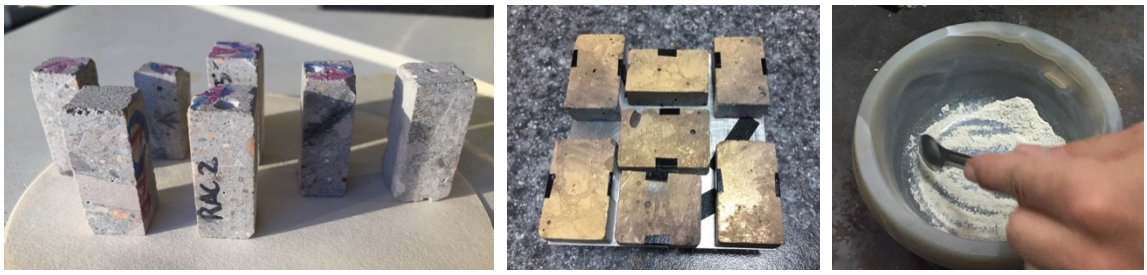

Fig. 1. *Concrete samples used for the μCT analysis (left), after the application of the gold coating for the SEM analysis (center) and crushing process of samples to 100 μm.*

3. Results and discussions

3.1. Physico-mechanical propierties

Table 2 presents the main physical and mechanical properties of the concrete mixes after 28 days of curing. Out of the physical properties, a slight increase in saturated surface dry (SSD) bulk specific gravity is highlighted, as a result of the higher amount of mortar incorporated in RA*i*. A slight decrease of apparent specific gravity associated with the number of recycling cycles is observed as a consequence of the increase in closed porosity, which occurs because of a higher volume of mortar. In any case, for less than three recycling cycles, the apparent specific gravity is higher than 2.5 g/cm^3.

209 ***Table 2.*** *Physical and mechanical properties of the control and recycled aggregate concrete obtained by*
210 *standard methods.*

Concrete mix	Bulk specific gravity	SSD bulk specific gravity	Apparent specific gravity	Open porosity [% vol.]	Absorption coefficient [% wt.]	Compressive strength [MPa]
SC	2.30	2.63	2.56	12.47	5.42	55.88
RAC1	2.16	2.59	2.53	16.81	7.78	54.21
RAC2	2.05	2.59	2.54	20.57	10.01	53.29
RAC3	2.08	2.64	2.46	20.97	10.05	48.65
RAC1-25	2.27	2.62	2.67	13.48	5.93	59.74
RAC2-25	2.25	2.60	2.58	13.41	5.94	55.77
RAC3-25	2.28	2.64	2.59	13.61	5.96	55.89

211
212 At the same time, a significant decrease in specific gravity was observed (Fig. 3), as a
213 consequence of the increase in accessible porosity, which is associated with the increasing volume of
214 mortar adhered to the original aggregate as the recycling cycles proceed. According to Thomas et al.
215 (Thomas et al., 2018), for this type of aggregate, the volume of adhered mortar increases 55%, 76% to
216 88% for cycles 1, 2 and 3 respectively. If the increase in open porosity is compared with the increase
217 of adhered mortar of the RA*i*, an excellent correlation is obtained (Fig. 2, on the right). This confirms
218 that the volume of new mortar in each RAC*i* at the time of mixing is the same, as a result of the same
219 aggregate volume in the mix and of the same porosity of the mortar. Thanks to this, it is possible to
220 identify the influence of the RA*i* on the RAC*i*. As the number of recycling increases, the volume of
221 mortar of the recycled concrete increases in an amount proportional to the volume of mortar adhered
222 that incorporates the recycled aggregate. Absolute values show higher increase in open porosity than
223 in the absorption coefficient but relative values show that the increase in weight is higher as a
224 consequence of the variation of water weight *versus* the variation of air volume. Guo et al. (Guo et al.,
225 2018) reported different factors that affect the properties of RAC, highlighting that the influence of
226 the adhered mortar volume is strongly negative. However, other authors proposed methods to
227 improve RA's properties that would have a higher influence on RA*i* with $i > 1$ than on single recycled
228 aggregate. For example, the CO_2 treatment proposed by Xuan et al. (Xuan et al., 2017; Zhan et al.,
229 2018) or scattering-filling aggregate method, decreasing the phenomenon of aggregate segregation
230 and increasing the coarse aggregate concentration to reduce the cement content, proposed by Xu et
231 al. (Xu et al., 2018) prevent the disadvantages of the properties of RA due to their higher porosity and
232 water absorption.
233

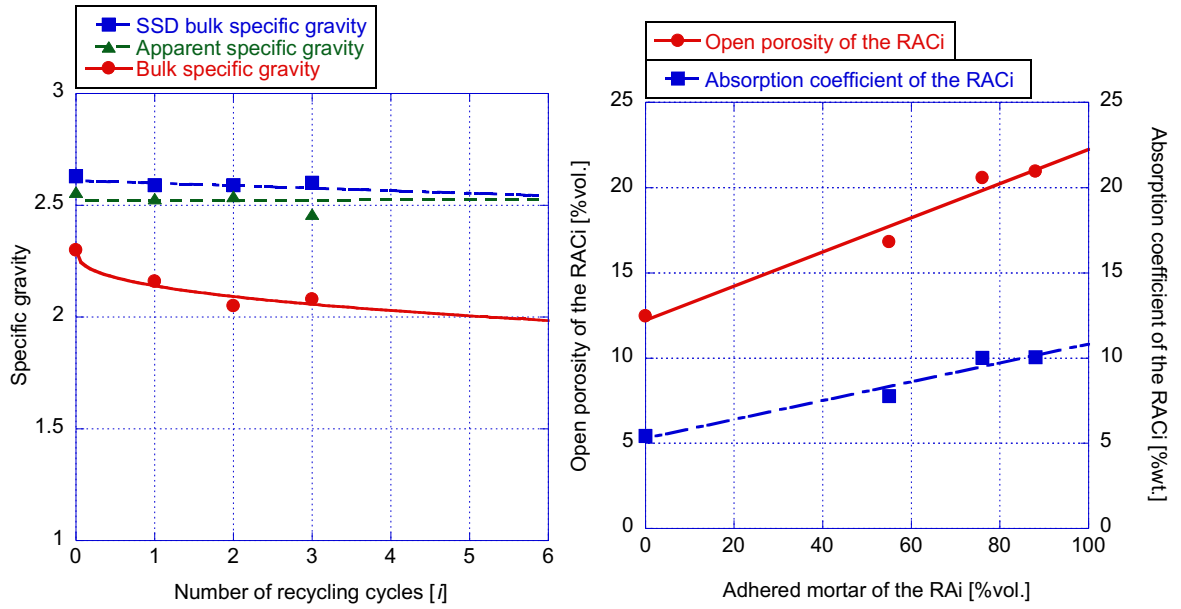

Fig. 2. *Physical properties of concrete vs. number of recycling cycles or adhered mortar content.*

At $i = 3$, the bulk specific gravity is nearing 2, i.e. a decrease of this parameter is expected as the coarse LA turns to sand as a result of the crushing process. At the moment, there are no results for a higher number of recycling cycles ($i > 3$) but it can be presumed that, after i cycles, when the LA in the RAi turns to a size smaller than 4 mm, the hardened RACi will have a composition equivalent to a mortar. According to Thomas et al.'s estimate (Thomas et al., 2018), the coarse LA turns to sand at $i = 6$. According to the trend line in Fig. 2, at $i = 6$ the concrete would have a specific gravity of 2 similar than that of a current mortar, so it is expected that the coarse LA turns completely to sand with 6 recycling cycles. As for open porosity and absorption coefficient, as seen in Fig. 3, they significantly increase in the first two recycling cycles and for $i > 2$ the increment is asymptotic, tending to an open porosity of 22%vol. and an absorption coefficient of 11%wt. Duan et al. (Duan and Poon, 2014) analyzed the influence of the adhered mortar content of different aggregates showing that, to produce RAC, a RA with good quality should have an apparent specific gravity over 2.5 g/cm^3, which corresponds to $i = 3$ in Fig. 3.

Fig. 3 shows how the LA progressively decreases in size, thus increasing the sand fraction. The sequence of the mixes with 100% incorporation is shown in the top row of Fig. 3, where the variation in LA size is more evident. For 25% substitution, the global decrease in the size of LA is not significant. RAC in all cases has the same aggregate grading but the LA fraction turns progressively into sand. Therefore, presumably by $i = 6$, all the RA will be made of hardened mortar and its incorporation as an aggregate in a mix, even though the mixing method, will produce rather a mortar than a concrete. The RACi sequence also shows that LA becomes not only smaller but also rounder.

In general, physical and mechanical properties are used as verification parameters in most structural concrete regulations. All results of the tests carried out in this section show that multi-recycled concrete has properties suitable for use as structural concrete. However, with each recycling, density and resistance are lost, so one of the great contributions of this paper is to quantify how much the loss is.

In general, physical and mechanical properties are used as verification parameters in most structural concrete standards. In this case, all physical and mechanical properties show that multi-recycled concrete has properties suitable for use as structural concrete. However, with each recycling, density and strength decrease, so the contribution of this paper is to quantify how much the loss per recycling is. On the other hand, physical and mechanical properties are not enough in themselves to guarantee the quality of multi-recycled concrete. An interesting research that would verify the conclusions proposed in this paper would be the analysis of the durability of the concrete. It is suggested to carry out in future capillary to gases and/or water tests because the greater volume of paste of the multi-recycled concrete could penalize its durability.

3.2. Computerized microtomography

Once the physico-mechanical properties of RAC*i* are obtained by standard methods, the proposed μCT method was validated and it was shown that highly interesting results can be obtained faster and easier.

Table 3 shows the results of the quantitative analysis by μCT. They confirm that for $i > 3$ the volume of coarse LA present in concrete is lower than 5% and that it turned almost completely to sand at $i = 6$ (Fig. 4). At the same time, the volume of cement and mortar paste found in concrete increases. The compaction index is the result of dividing the volume occupied by the aggregate by the total analysed volume. For SC and RAC*i* (i = *1, 2, 3*), the compaction index is 60.3%, 57.6%, 57.0% and 56.5% respectively (Thomas et al., 2018). Therefore, if the aggregate were tightly compacted in RAC*i*, the increase of adhered mortar within RA*i* should be in the interval 40-43 %vol. (100%- compaction index). Actually, the increase of mortar volume between SC and RAC1 is 25% and from RAC2 to RAC3 it is only 1.4%vol., which means that there is little volume that can be further converted to mortar after the third cycle.

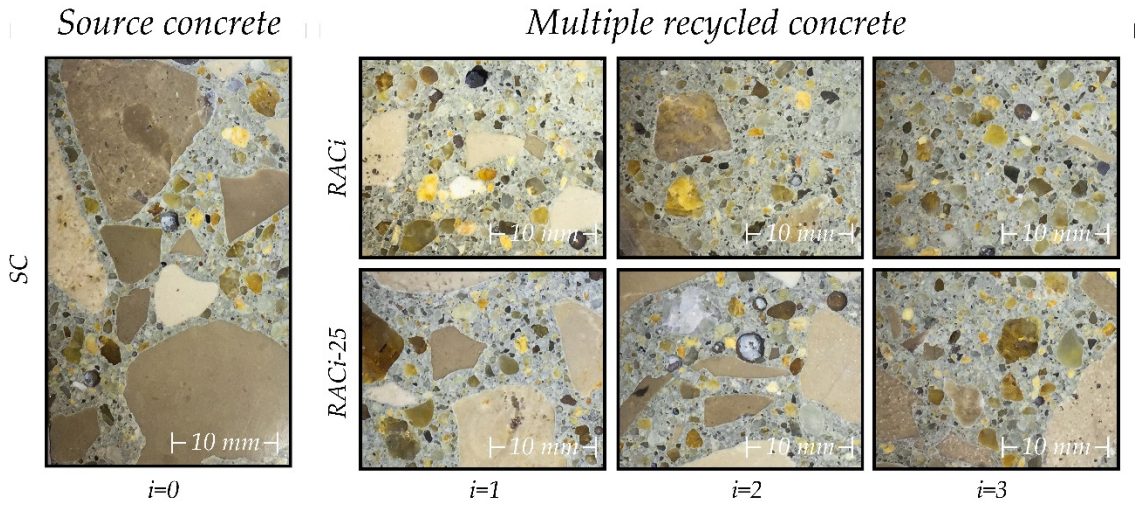

Fig. 3. *Macrograph details of an internal polished surface from the different concrete mixes studied.*

Table 3. *Properties of the control and recycled aggregate concrete obtained by μCT.*

Concrete mix	Coarse (> 4 mm) LA volume [% vol.]	Cement paste volume [% vol.]	Mortar volume [% vol.]	Closed porosity [% vol.]	LA/mortar ratio [% vol.]
SC	49.59	22.91	50.01	0.40	99.2
RAC1	22.66	48.75	75.85	0.76	29.9
RAC2	7.57	64.57	91.67	1.49	8.3
RAC3	5.14	65.94	93.04	1.81	5.5
RAC1-25	45.88	26.27	53.37	0.75	86.0
RAC2-25	43.15	27.09	54.19	0.43	79.6
RAC3-25	41.15	29.31	56.41	2.66	72.9

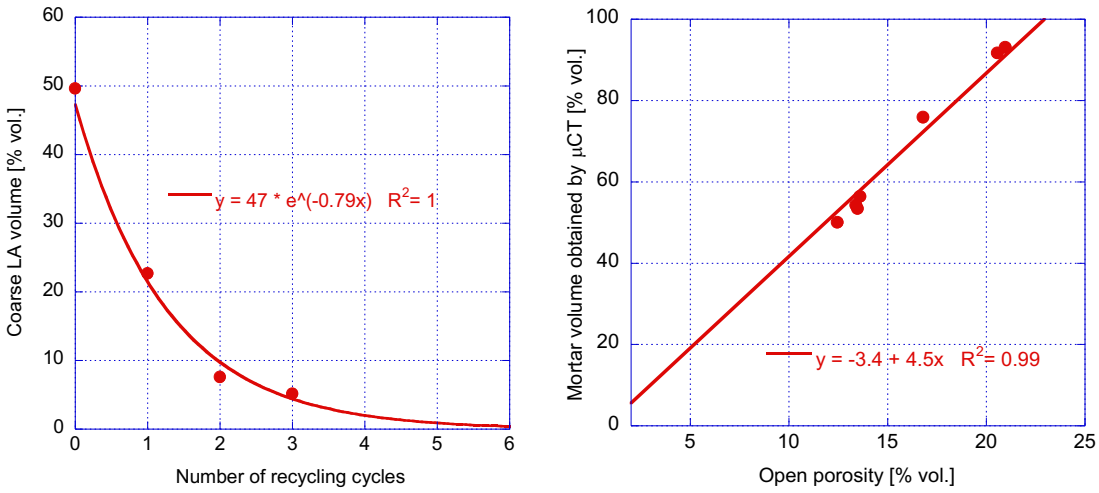

Fig. 4. *Volume of LA vs. number of recycling cycles (left) and mortar volume of concrete obtained by µCT vs. open porosity (right).*

According to previous research of Thomas et al. (Thomas et al., 2018), the closed porosity of RA*i* decreases with the number of cycles *i*; so the observed increase in closed porosity of concrete should be a consequence of the new cement paste. A similar effect has been found by Fiol et al. (Fiol et al., 2018) and Thomas et al. (Thomas et al., 2016) using RA from precast elements, external compaction and self-compacting concrete, showing that a higher volume of adhered mortar in RA influences negatively the physical and mechanical properties of concrete reducing the compressive strength a percentage that depends on the effective w/c ratio.

The correlation found in Fig. 4 between the concrete volume of mortar, obtained by µCT, and open porosity, obtained by standardized methods, demonstrates the reliability of µCT, and it also shows that it is possible to quickly predict the quality of the aggregate by determining the quantity of coarse LA both in the aggregate and in the concrete made with it.

Figs. 6 to 12 show the analyzed phases, coarse LA and closed porosity of the concrete mixes.

The sequence of closed porosity distribution on the right of each figure shows an increasing number of pores of RACi. At the same time, a reduction of the size of LA is reported. Finally, the distribution of closed porosity is progressively more homogeneous as i increases. For RAi, Thomas et al. (Thomas et al., 2018) reported similar decreases in the size of LA and a slight increase of the closed porosity with i. However, the increase of the closed porosity of concrete is mostly due to the new mortar of the RACi rather than to the increment of adhered mortar in the RAi. Another characteristic of the observed closed porosity is the sphericity of the pores and homogeneous distribution in the cement paste around the LA, also observed by Lanzón et al. (Lanzón et al., 2012). The efficiency of this technique depends on the difference of density of the phases of the components (Carrara et al., 2018). With multi-recycled aggregate, the density decreases and turns similar to the cement paste making not possible to differentiate old and new cement paste.

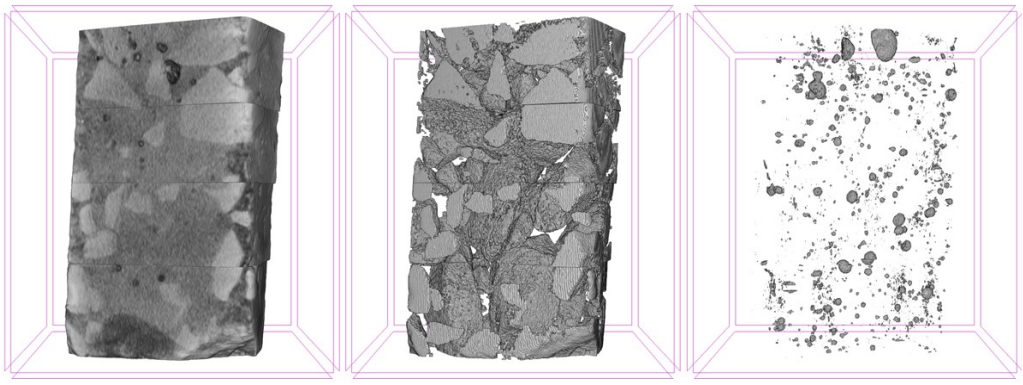

Fig. 5. *SC specimen (left), coarse LA in it (center) and its closed porosity (right).*

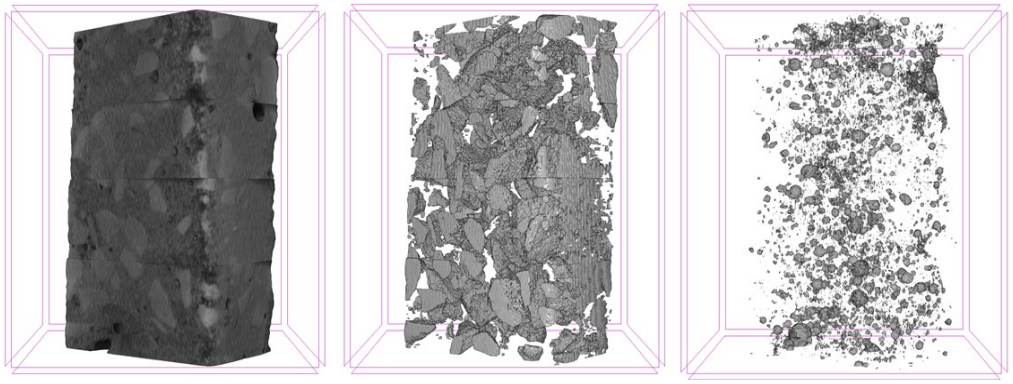

316
317 ***Fig. 6.*** *RAC1 specimen (left), coarse LA in it (center) and its closed porosity (right).*

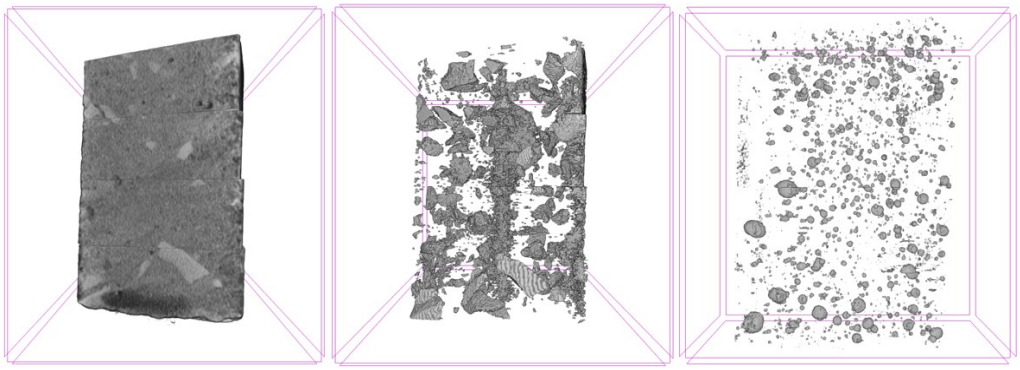

318
319 ***Fig. 7.*** *RAC2 specimen (left), coarse LA in it (center) and its closed porosity (right).*

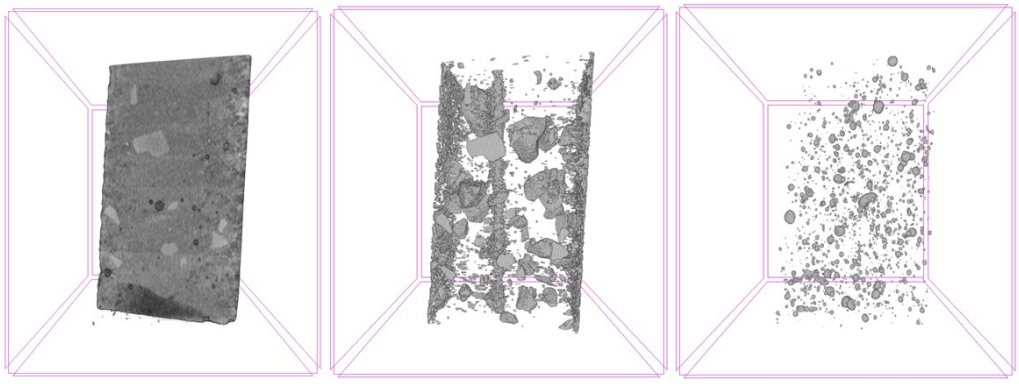

320
321 ***Fig. 8.*** *RAC3 specimen (left), coarse LA in it (center) and its closed porosity (right).*

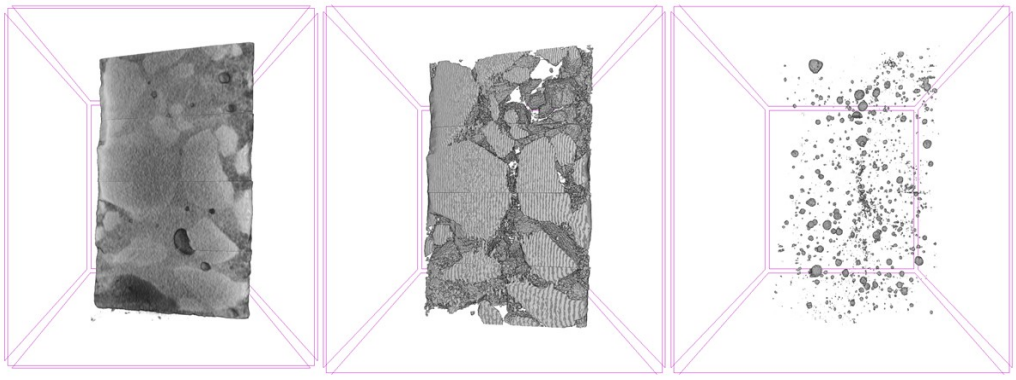

322
323 ***Fig. 9.*** *RAC1-25 specimen (left), coarse LA in it (center) and its closed porosity (right).*

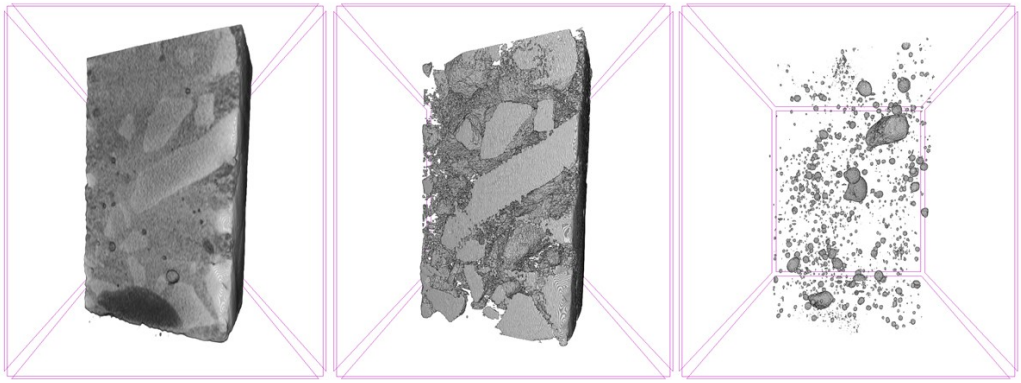

Fig. 10. *RAC2-25 specimen (left), coarse LA in it (center) and its closed porosity (right).*

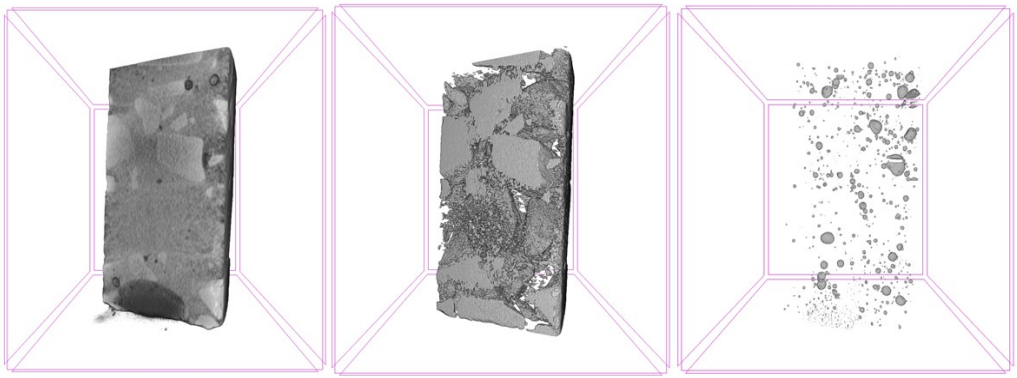

Fig. 11. *RAC3-25 specimen (left), coarse LA in it (center) and its closed porosity (right).*

In general, microtomography has been revealed as a very interesting mortar volume quantification technique. However, as there is still no standard regarding this type of characterization and comparisons with other research in which similar techniques are applied is complicated. A future work of interest would be to propose a standard or regulation regarding the test parameters since the numerical results of this technique are influenced by these adjustments.

3.3. Scan electron microscopy

Table 4 shows the elemental chemical composition of the control and recycled aggregate concrete mixes. Its analysis shows a clear decrease in the amount of C and Ca while the content of Al, S and Fe increases. The decrease of C and Ca is due to the decrease of both the size and the amount of limestone aggregate ($CaCO_3$) as *i* increases. In fact, the increase in the amount of Si, S and Fe is due to the increase of the volume of mortar with the number of recycling cycles.

Table 4. *Elemental chemical composition of the control and recycled aggregate concrete obtained by SEM.*

Elem.	Quant.	SC	RAC1	RAC2	RAC3	RAC1-25	RAC2-25	RAC3-25
O	%Atm.	65.85	61.97	63.14	66.68	63.54	63.24	60.36
	%Wt.	54.01	51.58	53.56	53.34	52.31	53.05	51.53
C	%Atm.	16.57	19.49	19.13	11.09	17.59	18.29	21.48
	%Wt.	10.2	12.18	12.18	6.66	10.87	11.52	13.77
Si	%Atm.	0.25	3.08	4.25	5.93	2.87	4.51	5.13
	%Wt.	0.36	4.49	6.32	8.33	4.14	6.64	7.69
Ca	%Atm.	17.11	13.93	11.52	13.6	15.52	12.97	11.33
	%Wt.	35.15	29.04	24.47	27.26	32	27.26	24.23
Mg	%Atm.	0.22	0.3	0.27	0.39	-	-	-

Elem.	Quant.	SC	RAC1	RAC2	RAC3	RAC1-25	RAC2-25	RAC3-25
	%Wt.	0.27	0.37	0.34	0.48	-	-	-
Al	%Atm.	-	0.51	0.72	1.12	0.49	0.79	0.96
	%Wt.	-	0.72	1.02	1.51	0.67	1.11	1.38
S	%Atm.	-	0.23	0.4	0.44	-	-	0.37
	%Wt.	-	0.38	0.67	0.71	-	-	0.64
K	%Atm.	-	0.23	0.36	0.4	-	0.2	0.37
	%Wt.	-	0.47	0.74	0.79	-	0.42	0.77
Fe	%Atm.	-	0.26	0.23	0.33	-	-	-
	%Wt.	-	0.77	0.69	0.92	-	-	-

Elements such as Al or Fe could be used as indicators of the quality of the RA*i*, and in general terms of RA. The SC mix, with 350 kg/m^3 of Portland CEM I cement, does not show a significant amount of these elements, compared to the others. However, as the cement paste present in concrete and the amount of Al and Fe increases, the latter become significant and can be associated with the volume of mortar adhered and, consequently, with the quality of RA. It is a fast and simple way to compare the quality of RA and it can be used as a standard method to classify the adequacy of RA.

Figs. 13 to 16 show the secondary electron micrograph sequence at 50, 100, 500 and 1500 magnification of the SC, RAC1, RAC2 and RAC3 mixes. Figs. 17 to 19 show the micrograph sequence at 50, 100, 500 and 1000 magnification of the RAC1-25, RAC2-25 and RAC3-25 mixes.

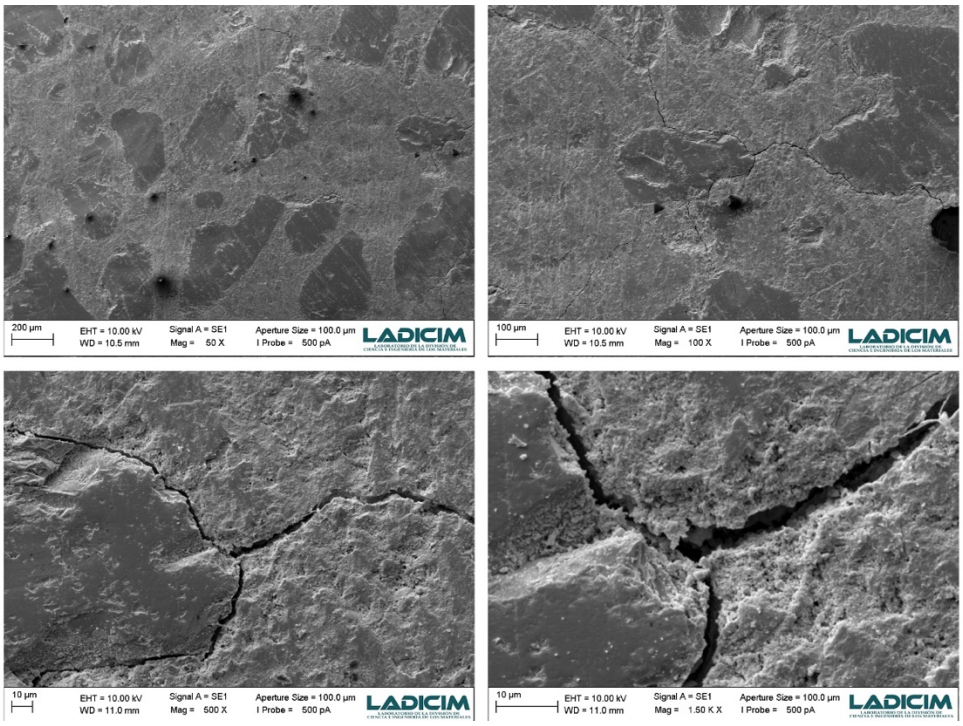

Fig. 12. *Scan electron micrograph sequence (50x, 100x, 500x and 1500x) of a region of aggregate-cement paste interphase of SC.*

In the micrographs relative to SC (Fig. 12), a dense cement paste is observed. In the analyzed area, a few bubbles of retained air are observed. Since SC has not been subjected to any deterioration process, the small fissures observed must have resulted from a shrinkage process. No propagation of fissures occurs through the LA particles. The main path of fissures is through the interfacial transition zone (ITZ), causing the failure of the cement paste-aggregate binding. Fissures through the cement paste are also observed. In this case, the fissure propagates from one LA particle to another,

corresponding to an inter-aggregate propagation mode (InterPM) using the shortest path. The maximum measured fissure size in SC is 4 μm. The fissures observed in the first recycling do not appear in the second one because they will be the weak points from which the concrete is crushed in the process of recycling.

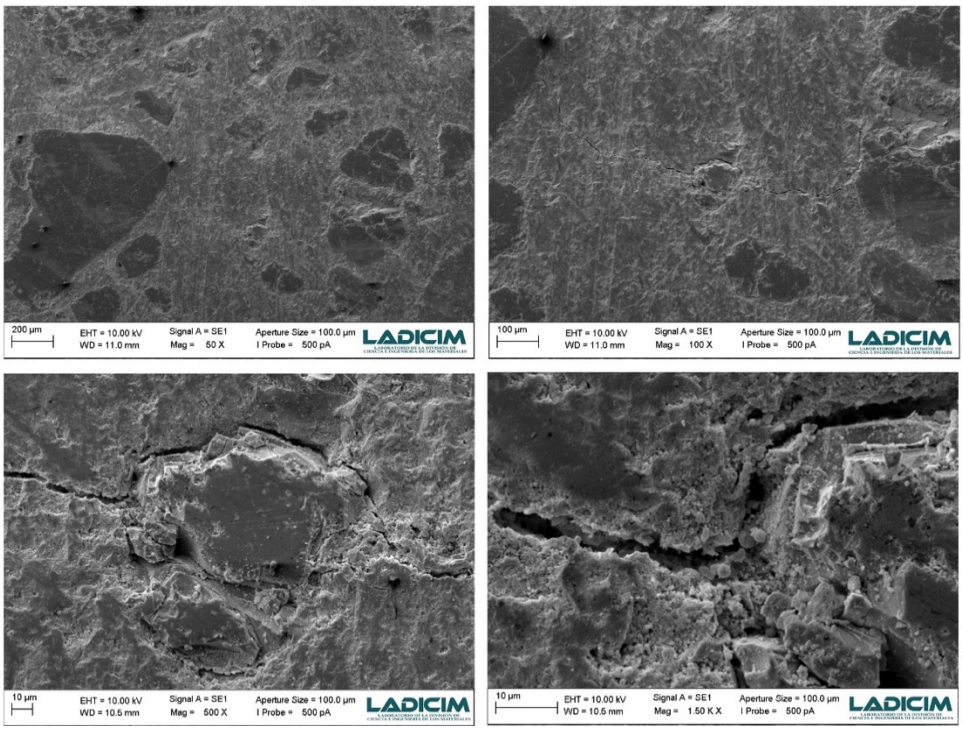

Fig. 13. *Scan electron micrograph sequence (50x, 100x, 500x and 1500x) of a region of aggregate-cement paste interphase of RAC1.*

In RAC1 (Fig. 13), as in SC, a dense cement paste with few pores are observed. Again, the main propagation of fissures is through the ITZ, between cement paste and LA, but secondary fissures through the cement paste are observed. InterPM is not observed. This propagation path of the fissures results from the only one damage mechanism detected in the samples, which means that the ITZ between new and old cement paste is not less resistant than the paste itself. The presence of fissures in RAC1 can be explained in two ways: shrinkage of the RAC1's paste or the previous fissures in RA1. Only few fissures are observed because, in the crushing process of the SC, the weakest fissures are eliminated when the concrete breaks through them. The maximum measured fissure size in the analyzed area of RAC1 is 3 μm.

In RAC2 (Fig. 14), the cement paste seems quite similar to that of SC and RAC1, with a dense structure. In this case, more fissures seem to propagate through the cement paste than in SC and RAC1. The existence of two concrete pastes leads to fissures caused by shrinkage of the old cement paste (in RA2) and the new one (from RAC2 itself) and the previous fissures in RA2. The maximum measured fissure size in the analyzed area of RAC2 is 4.5 μm.

In RAC3 (Fig. 15), a dense cement paste is observed. In this case, the same as in RAC2 mechanisms of fissure propagation are detected in the analyzed area, i.e. mainly through the ITZ and secondarily through the cement paste. The maximum measured fissure size in the analyzed area of RAC3 is 3.5 μm.

In RAC1-25 (Fig. 16), as expected, a dense cement paste with few pores is observed. Fissures propagate through the ITZ and from one aggregate to the next one, following the shortest way between them. In the analyzed area, the maximum fissure size is similar to the one found in RAC2. However, the crack density is slightly higher. Most of the fissures are associated with the interface between cement paste and aggregate. Not only does the size of natural aggregates decreases but their presence is also minimized. Consequently, the more deformable RCA, composed mostly of old

adhered mortar, present a lower capacity to restrain the shrinkage of concrete and thus greater deformation is observed.

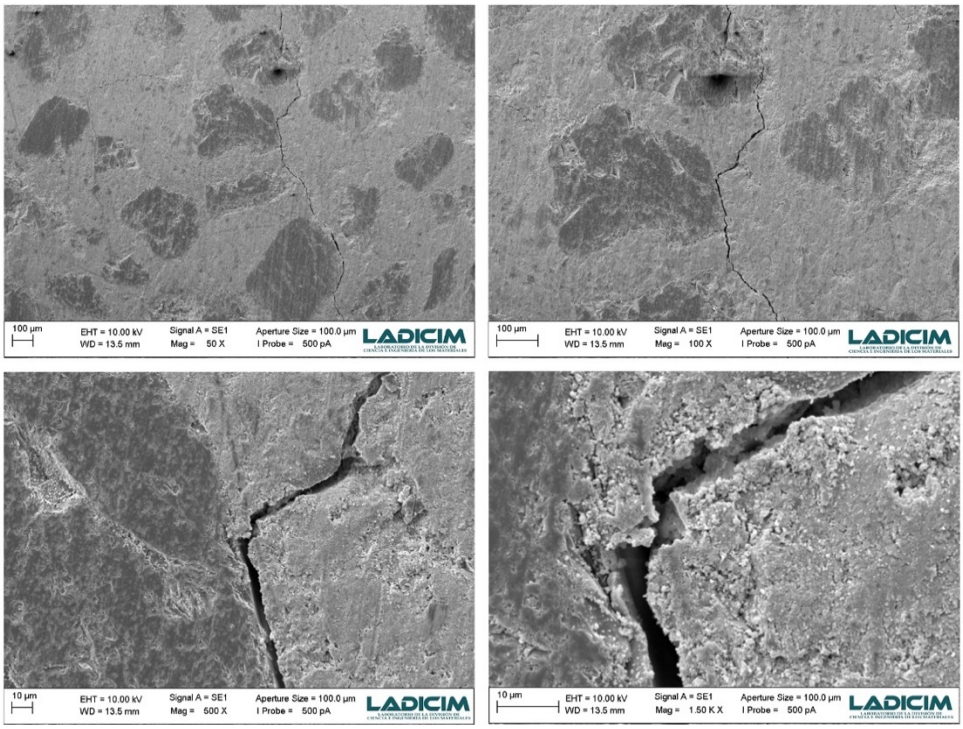

Fig. 14. *Scan electron micrograph sequence (50x, 100x, 500x and 1500x) of a region of aggregate-cement paste interphase of RAC2.*

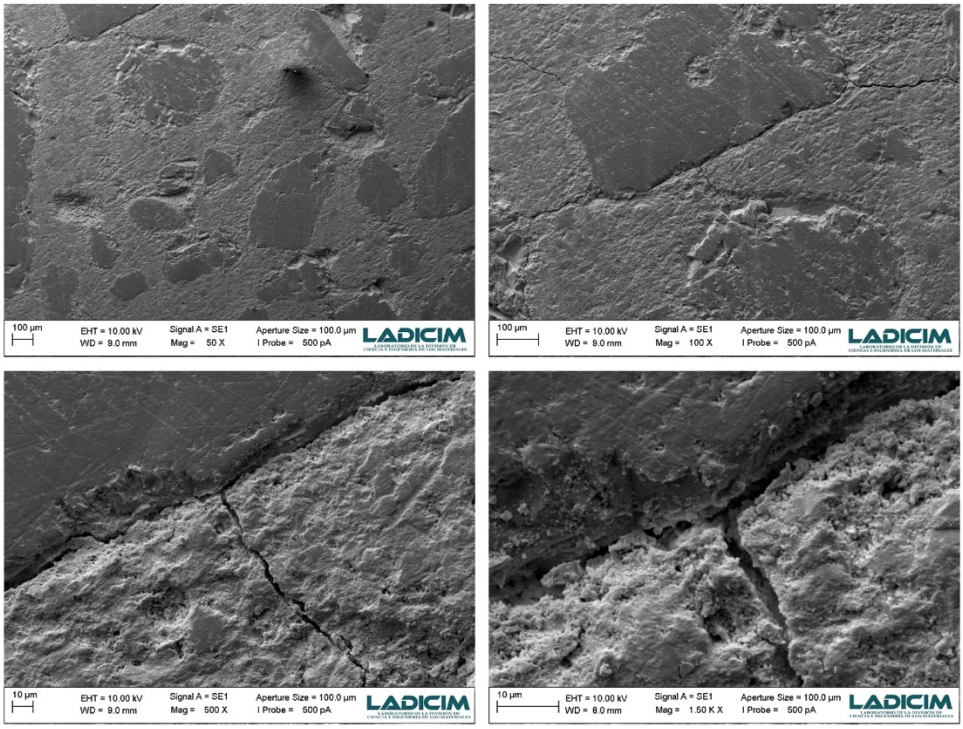

Fig. 15. *Scan electron micrograph sequence (50x, 100x, 500x and 1500x) of a region of aggregate-cement paste interphase of RAC3.*

In RC2-25 (Fig. 17), the propagation of fissures occurs through the ITZ and the cement paste in the inter-aggregate fissures. The maximum measured fissure size is 1.5 µm.

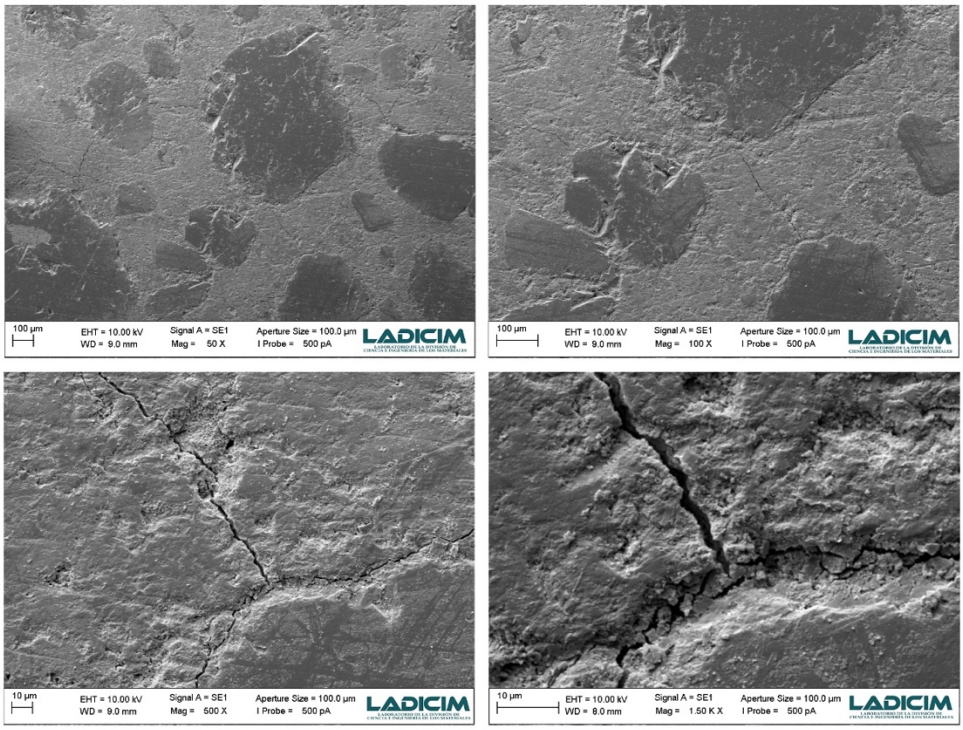

Fig. 16. *Scan electron micrograph sequence (50x, 100x, 500x and 1500x) of aggregate-cement paste interphase of RAC1-25.*

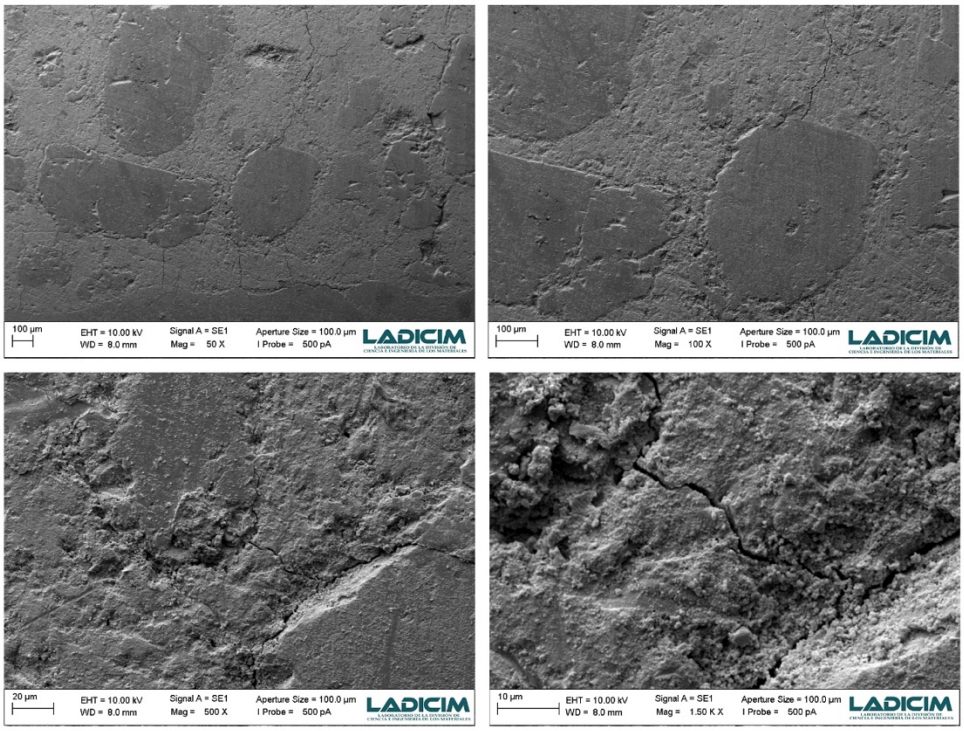

Fig. 17. *Scan electron micrograph sequence (50x, 100x, 500x and 1500x) of aggregate-cement paste interphase of RAC2-25.*

In the analyzed area of RAC3-25 (Fig. 18), a greater amount of cement paste and a greater separation between LA is observed than in RC2-25 but the same mechanisms of fissure propagation

occur. In areas of greater concentration of cement paste, the fissures' path follows the ITZ of the small aggregates. The maximum measured fissure size in RAC3-25 is 4 μm.

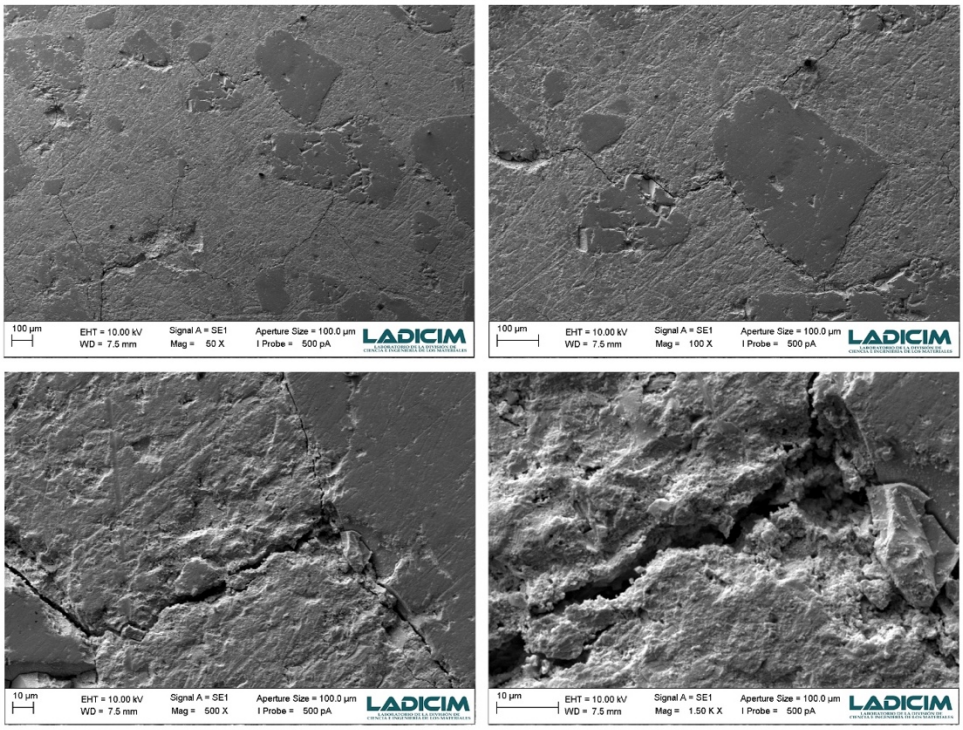

Fig. 18. *Scan electron micrograph sequence (50x, 100x, 500x and 1500x) of aggregate-cement paste interphase of RAC3-25.*

With the SEM analysis, it is demonstrated that the higher content of cement paste incorporated in the aggregate and the reduction of the size of LA have negative effects on the microstructure of RAC, as was also reported by Sáez del Bosque et al. (Medina et al., 2012; Sáez del Bosque et al., 2017).

Electron microscopy facilitates the understanding of the mechanisms that affect the properties of multi-recycled concrete. However, it is practically impossible to distinguish old mortar from new one when the multi-recycled concrete is prepared with the same proportions. We propose a future research in which a different chemical tracer is incorporated into each of the multi-recycled concretes allowing to identify to which generation of recycling the mortar belongs. For example, by incorporating some heavy elements in a proportion to be detected by the EDS but small enough that it does not affect the properties of the concrete, they would show the the distribution of different mortars into the 3th generation recycled concrete.

4. Conclusions

From the study of the physical properties by standard methods, the obtained parameters using microtomography and the microstructural qualitative observations of multi-recycled aggregate concrete mixes, the following conclusions can be drawn:

- Regarding physical properties, the loss of density and increase in closed porosity as the recycling cycles is a consequence of the increase of attached mortar in the multi-recycled aggregate and of the reduction in size of the natural fraction of the aggregate with the recycling cycles. Mixes with higher ratios of natural coarse aggregate will thus produce recycled aggregates that will retain their characteristics for a bigger number of cycles.

- Based on the results of microtomography, the closed porosity of recycled aggregate decreases but it increases in the resulting multi-recycled aggregate concrete with the number of recycling cycles. The reliability of the method has been demonstrated and makes it possible to quickly predict the quality of the aggregate by measuring the volume of the coarse natural fraction of the aggregate.

- The analysis of the chemical elemental composition of the multi-recycled aggregate concrete shows that the Al and Fe concentration increases with the number of recycling cycles, which can be associated with the volume of adhered mortar and, consequently, with the quality of the recycled aggregate. This analysis is a fast and simple method to evaluate quantity of cement in the recycled aggregates.

- The observed trend curves show that the coarse natural fraction of the recycled aggregate turns to sand after 5-6 recycling cycles. If recycled aggregate with more than 5 cycles is incorporated in the mix, a mortar rather than a concrete will be obtained. There is a dependence between the recycled aggregate production process and the lifespan of the multi-recycled aggregate concrete because, if small-size recycled aggregate is produced in the crushing process, the size of the natural aggregate fraction will be smaller and, as a consequence, the multi-recycled aggregate concrete will become a mortar in a smaller number of cycles.

- The microstructural analysis reveals the presence of fissures due to the shrinkage of the concrete. The greater presence of mortar in multi-recycled concretes causes a greater number of shrinkage fissures to appear. However, the size of the fissures is similar in all multi-recycled concrete mixes. No fissure generated in a new-old cement paste interface has been observed. All the fissures are generated in the cement paste-natural aggregate interface, regardless of their origin.

As future research, we recommend to carry out capillary to gases and/or water tests because the greater volume of paste of the multi-recycled concrete could penalize its durability. Also, research to propose a standard or regulation regarding the microtomography test parameters since the numerical results of this technique are influenced by these adjustments. Finally, regarding the microstructural analysis, incorporating some heavy elements in a proportion to be detected by EDS but small enough that it does not affect the properties of the concrete, they would show the the distribution of different mortars into the 3th generation recycled concrete.

Acknowledgments

The authors would like to thank:

To the LADICIM, Laboratory of Materials Science and Engineering of the University of Cantabria and Instituto Superior Técnico of the University of Lisbon for making available to the authors the facilities used in this research.

To the José Castillejo Program, founded by the Ministry of Science, Innovation and Universities of Spain, for the research stay of Carlos Thomas at the CERIS, Instituto Superior Técnico of the University of Lisbon, Portugal.

References

12390-3, E.N., 2009. Testing hardened concrete - Part 3: Compressive strength of test specimens.

12390-4, E.N., 2001. Testing hardened concrete - Part 4: Compressive strength - Specification for testing machines.

ANEFA, 2017. Estadisticas de la Asociación Nacional de Empresarios Fabricantes de Áridos.

Asahina, D., Landis, E.N., Bolander, J.E., 2011. Modeling of phase interfaces during pre-critical crack growth in concrete. Cem. Concr. Compos. https://doi.org/https://doi.org/10.1016/j.cemconcomp.2011.01.007

Brito, J. de, Agrela, F., Silva, R.V., 2019. Chapter 1: Construction and demolition waste. New Trends in Eco-efficient and Recycled Concrete.

Buck, A.D., 1973. RECYCLED CONCRETE. Highw Res Rec 1–8. https://doi.org/https://doi.org/10.1016/j.cemconres.2007.02.002

Carrara, P., Kruse, R., Bentz, D.P., Lunardelli, M., Leusmann, T., Varady, P.A., De Lorenzis, L., 2018. Improved mesoscale segmentation of concrete from 3D X-ray images using contrast enhancers. Cem. Concr. Compos. https://doi.org/https://doi.org/10.1016/j.cemconcomp.2018.06.014

484 Chotard, T.J., Boncoeur-Martel, M.P., Smith, A., Dupuy, J.P., Gault, C., 2003. Application of X-ray
485 computed tomography to characterise the early hydration of calcium aluminate cement. Cem.
486 Concr. Compos. 25, 145–152. https://doi.org/10.1016/S0958-9465(01)00063-4
487 Duan, Z.H., Poon, C.S., 2014. Properties of recycled aggregate concrete made with recycled
488 aggregates with different amounts of old adhered mortars. Mater. Des.
489 https://doi.org/https://doi.org/10.1016/j.matdes.2014.01.044
490 EN-12390-7, 2009. Testing hardened concrete - Part 7: Density of hardened concrete.
491 Etxeberria, M., Vázquez, E., Marí, A., Barra, M., 2007. Influence of amount of recycled coarse
492 aggregates and production process on properties of recycled aggregate concrete. Cem. Concr.
493 Res. 37, 735–742. https://doi.org/10.1016/j.cemconres.2007.02.002
494 Evangelista, L., de Brito, J., 2007. Mechanical behaviour of concrete made with fine recycled concrete
495 aggregates. Cem. Concr. Compos. 29, 397–401.
496 https://doi.org/10.1016/J.CEMCONCOMP.2006.12.004
497 Fiol, F., Thomas, C., Muñoz, C., Ortega-López, V., Manso, J.M., 2018. The influence of recycled
498 aggregates from precast elements on the mechanical properties of structural self-compacting
499 concrete. Constr. Build. Mater. 182, 309–323. https://doi.org/10.1016/j.conbuildmat.2018.06.132
500 Guo, H., Shi, C., Guan, X., Zhu, J., Ding, Y., Ling, T.-C., Zhang, H., Wang, Y., 2018. Durability of
501 recycled aggregate concrete – A review. Cem. Concr. Compos.
502 https://doi.org/https://doi.org/10.1016/j.cemconcomp.2018.03.008
503 Kou, S.C.S.S.C., Poon, C.S.S., 2012. Enhancing the durability properties of concrete prepared with
504 coarse recycled aggregate. Constr. Build. Mater. 35, 69–76.
505 https://doi.org/10.1016/J.CONBUILDMAT.2012.02.032
506 Kwan, W.H., Ramli, M., Kam, K.J., Sulieman, M.Z., 2012. Influence of the amount of recycled coarse
507 aggregate in concrete design and durability properties. Constr. Build. Mater. 26, 565–573.
508 https://doi.org/https://doi.org/10.1016/j.conbuildmat.2011.06.059
509 Lanzón, M., Cnudde, V., de Kock, T., Dewanckele, J., 2012. X-ray microtomography (μ-CT) to
510 evaluate microstructure of mortars containing low density additions. Cem. Concr. Compos.
511 https://doi.org/https://doi.org/10.1016/j.cemconcomp.2012.06.011
512 López Gayarre, F., Suárez González, J., Blanco Viñuela, R., López-Colina Pérez, C., Serrano López,
513 M.A., 2018. Use of recycled mixed aggregates in floor blocks manufacturing. J. Clean. Prod. 167,
514 713–722. https://doi.org/10.1016/j.jclepro.2017.08.193
515 Medina, C., Frías, M., de Rojas, M.I.S., 2012. Microstructure and properties of recycled concretes using
516 ceramic sanitary ware industry waste as coarse aggregate. Constr. Build. Mater. 31, 112–118.
517 https://doi.org/https://doi.org/10.1016/j.conbuildmat.2011.12.075
518 Meyer, C., 2009. The greening of the concrete industry. Cem. Concr. Compos. 31, 601–605.
519 https://doi.org/10.1016/J.CEMCONCOMP.2008.12.010
520 Monteiro, P.J.M., Kirchheim, A.P., Chae, S., Fischer, P., MacDowell, A.A., Schaible, E., Wenk, H.R.,
521 2009. Characterizing the nano and micro structure of concrete to improve its durability. Sustain.
522 Civ. Eng. Struct. - Durab. Concr.
523 https://doi.org/https://doi.org/10.1016/j.cemconcomp.2008.12.007
524 Oneschkow, N., 2016. Fatigue behaviour of high-strength concrete with respect to strain and stiffness.
525 Int. J. Fatigue 87, 38–49. https://doi.org/http://dx.doi.org/10.1016/j.ijfatigue.2016.01.008
526 Pedro, D., de Brito, J., Evangelista, L., 2017. Mechanical characterization of high performance concrete

prepared with recycled aggregates and silica fume from precast industry. J. Clean. Prod. 164, 939–949. https://doi.org/10.1016/j.jclepro.2017.06.249

Sáez del Bosque, I.F., Zhu, W., Howind, T., Matías, A., Sánchez de Rojas, M.I., Medina, C., 2017. Properties of interfacial transition zones (ITZs) in concrete containing recycled mixed aggregate. Cem. Concr. Compos. https://doi.org/https://doi.org/10.1016/j.cemconcomp.2017.04.011

Salesa, Á., Pérez-Benedicto, J.Á., Esteban, L.M., Vicente-Vas, R., Orna-Carmona, M., 2017. Physico-mechanical properties of multi-recycled self-compacting concrete prepared with precast concrete rejects. Constr. Build. Mater. 153, 364–373. https://doi.org/10.1016/j.conbuildmat.2017.07.087

Silva, R. V, De Brito, J., Dhir, R.K., 2014. Properties and composition of recycled aggregates from construction and demolition waste suitable for concrete production. Constr. Build. Mater. 65, 201–217.

Texas A&M Transportation Institute. PUBL.WKS, 1972. Recycling rubble for highway purposes. PUBL.WKS.

Thomas, C., Carrascal, I., Setién, J., Polanco, J.A., 2009. Determinación del límite a fatiga en hormigones reciclados de aplicación estructural - Determining the fatigue limit recycled concrete structural application (In Spanish). An. Mecánica la Fract. 1, 283–289.

Thomas, C., de Brito, J., Gil, V., Sainz-Aja, J.A., Cimentada, A., 2018. Multiple recycled aggregate properties analysed by X-ray microtomography. Constr. Build. Mater. 166, 171–180. https://doi.org/10.1016/J.CONBUILDMAT.2018.01.130

Thomas, C., Setién, J., Polanco, J.A.A., 2016. Structural recycled aggregate concrete made with precast wastes. Constr. Build. Mater. 114, 536–546. https://doi.org/10.1016/j.conbuildmat.2016.03.203

Thomas, C., Setién, J., Polanco, J.A.A., Lombillo, I., Cimentada, A., 2014. Fatigue limit of recycled aggregate concrete. Constr. Build. Mater. 52, 146–154. https://doi.org/10.1016/J.CONBUILDMAT.2013.11.032

Thomas, C., Setién, J., Polanco, J.A.Ja., Alaejos, P., De Juan, M.S., Sánchez de Juan, M., 2013. Durability of recycled aggregate concrete. Constr. Build. Mater. 40, 1054–1065. https://doi.org/10.1016/J.CONBUILDMAT.2012.11.106

Xiao, J., Li, J., Zhang, C., 2005. Mechanical properties of recycled aggregate concrete under uniaxial loading. Cem. Concr. Res. 35, 1187–1194. https://doi.org/https://doi.org/10.1016/j.cemconres.2004.09.020

Xu, G., Shen, W., Zhang, B., Li, Y., Ji, X., Ye, Y., 2018. Properties of recycled aggregate concrete prepared with scattering-filling coarse aggregate process. Cem. Concr. Compos. https://doi.org/https://doi.org/10.1016/j.cemconcomp.2018.06.013

Xuan, D., Zhan, B., Poon, C.S., 2017. Durability of recycled aggregate concrete prepared with carbonated recycled concrete aggregates. Cem. Concr. Compos. 84, 214–221. https://doi.org/10.1016/j.cemconcomp.2017.09.015

Zhan, B.J., Xuan, D.X., Poon, C.S., 2018. Enhancement of recycled aggregate properties by accelerated CO2 curing coupled with limewater soaking process. Cem. Concr. Compos. 89, 230–237. https://doi.org/10.1016/j.cemconcomp.2018.03.011